NHERF1 Is Required for Localization of PMCA2 and Suppression of Early Involution in the Female Lactating Mammary Gland

Jaekwang Jeong,[1] Wonnam Kim,[2] Julie Hens,[1] Pamela Dann,[1] Pepper Schedin,[3] Peter A. Friedman,[4] and John J. Wysolmerski[1]

[1]Section of Endocrinology and Metabolism, Department of Medicine, Yale University School of Medicine, New Haven, Connecticut 06510; [2]Division of Pharmacology, College of Korean Medicine, Semyung University, Jecheon 27136, Republic of Korea; [3]Department of Cell, Developmental, and Cancer Biology, Oregon Health and Science University, Portland, Oregon 97239; and [4]Department of Pharmacology and Chemical Biology, University of Pittsburgh School of Medicine, Pittsburgh, Pennsylvania 15260

ORCiD numbers: 0000-0001-8865-2545 (J. Jeong).

Prior studies have demonstrated that the calcium pump, plasma membrane calcium ATPase 2 (PMCA2), mediates calcium transport into milk and prevents mammary epithelial cell death during lactation. PMCA2 also regulates cell proliferation and cell death in breast cancer cells, in part by maintaining the receptor tyrosine kinase ErbB2/HER2 within specialized plasma membrane domains. Furthermore, the regulation of PMCA2 membrane localization and activity in breast cancer cells requires its interaction with the PDZ domain–containing scaffolding molecule sodium-hydrogen exchanger regulatory factor (NHERF) 1. In this study, we asked whether NHERF1 also interacts with PMCA2 in normal mammary epithelial cells during lactation. Our results demonstrate that NHERF1 expression is upregulated during lactation and that it interacts with PMCA2 at the apical membrane of secretory luminal epithelial cells. Similar to PMCA2, NHERF1 expression is rapidly reduced by milk stasis after weaning. Examining lactating NHERF1 knockout (KO) mice showed that NHERF1 contributes to the proper apical location of PMCA2, for proper apical–basal polarity in luminal epithelial cells, and that it participates in the suppression of Stat3 activation and the prevention of premature mammary gland involution. Additionally, we found that PMCA2 also interacts with the closely related scaffolding molecule, NHERF2, at the apical membrane, which likely maintains PMCA2 at the plasma membrane of mammary epithelial cells in lactating NHERF1KO mice. Based on these data, we conclude that, during lactation, NHERF1 is required for the proper expression and apical localization of PMCA2, which, in turn, contributes to preventing the premature activation of Stat3 and the lysosome-mediated cell death pathway that usually occur only early in mammary involution. (***Endocrinology*** **160: 1797–1810, 2019)**

In mammals, reproductive cycles are associated with the proliferation and differentiation of a large number of secretory alveolar epithelial cells during pregnancy (1–4). During lactation, these cells produce milk to feed offspring but, once no longer needed after weaning, they are eliminated in a two-stage process of coordinated cell death (3–5). The first phase of mammary involution is triggered by milk collecting in the alveolar lumens (milk stasis), and the second phase is triggered by the drop in circulating prolactin levels (3–5). Regulation of the involution process is very complex and involves the participation of many signaling molecules and cell types. However, a dominant pathway triggering the first phase of involution involves the activation and nuclear translocation of the transcription factor Stat3 (2–4). Milk stasis causes distension of the alveolar lumen, changing

ISSN Online 1945-7170

Received 22 March 2019. Accepted 7 May 2019.
First Published Online 14 May 2019

Abbreviations: ERM, ezrin/radixin/moesin/merlin; H&E, hematoxylin and eosin; JAK1, Janus kinase 1; KO, knockout; LIF, leukemia inhibitory factor; NHERF, sodium–hydrogen exchanger regulatory factor; PDZ, PSD-95/*Drosophila* discs large/ZO-1; phospho-, phosphorylated; PLA, proximity ligation assay; PMCA2, plasma membrane calcium ATPase 2; qPCR, quantitative PCR; TBST, Tris-buffered saline with 1% Tween 20; WGA, wheat germ agglutinin; WT, wild-type.

the shape of the mammary epithelial cells and upregulating the production of leukemia inhibitory factor (LIF), which, in turn, activates its receptor and Janus kinase 1 (JAK1), leading to phosphorylation of Stat3. Phosphorylated (phospho-)Stat3, in turn, activates a process of lysosomal biogenesis and reuptake of milk lipids causing increased permeability of the lysosomal membranes and activation of a cathepsin-mediated form of caspase-negative cell death (6, 7). The dying cells are either shed into the lumen, where they become TUNNEL positive, or are phagocytosed by their neighboring viable epithelial cells. Although this process is reversible when suckling is resumed within 48 hours, beyond that time, systemic prolactin levels decline, which then leads to activation of matrix metalloproteinases, irreversible breakdown of the basement membrane, and a wave of more widespread cell death by apoptosis (3, 4).

The plasma membrane calcium ATPase 2 (PMCA2) is a P-type ion pump that transports calcium from the cytoplasm across the plasma membrane and into the extracellular fluid (8–10). It is highly expressed at the apical surface of lactating breast cells, where it transports calcium into milk (11–13). Its expression rapidly decreases after weaning in response to milk stasis, and lactating PMCA2-null mice display premature activation of mammary involution associated with elevated intracellular calcium levels. PMCA2 is also re-expressed in breast cancers, and in HER2-positive breast cancer cells it interacts with several scaffolding molecules and HSP90 to maintain active HER2–Akt signaling, which is important for cell proliferation and survival (14, 15).

The sodium–hydrogen exchanger regulatory factor (NHERF) 1 is one of a family of four scaffolding proteins (NHERF1 to NHERF4) that contain tandem PSD-95/*Drosophila* discs large/ZO-1 (PDZ) domains and a C-terminal ezrin/radixin/moesin/merlin (ERM) binding domain (16–20). NHERF1 interacts with a variety of membrane proteins such as ion channels/transporters, G-protein–coupled receptors, and receptor tyrosine kinases through interactions with a canonical PDZ binding motif, which allows it to facilitate the formation of multiprotein signaling complexes that are tethered to the actin cytoskeleton (16–20). NHERF1 has been reported to participate in the initiation and maintenance of apical/basal polarity in polarized cells, where it is found at the apical cell membrane (21, 22). In surface epithelial cells, it also facilitates the structural organization of microvilli at the apical surface as well as the retention of signaling complexes within microvilli (23–27).

NHERF1 has been reported to be expressed in breast epithelial and breast cancer cells and to have variable functions (28–37). In the normal mammary gland, NHERF1 has been shown to be expressed at low levels at the apical surface of ductal mammary epithelial cells of virgin mice (24, 38). During lactation, NHERF1 expression is upregulated, and Morales *et al.* (38) have reported that it becomes expressed at the basolateral surface of secretory epithelial cells in the mouse mammary gland. They reported that NHERF1 interacted with the prolactin receptor and was necessary for proper prolactin-induced Stat5 signaling as well as secretory differentiation of mammary epithelial cells (38). NHERF1 expression is also upregulated in many breast cancers, and different NHERF1 mutations have been reported either to inhibit or to promote breast cancer cell growth (30, 36, 39–41). In several studies, tumor NHERF1 levels have been shown to correlate with HER2 expression (24, 28, 33, 34), and in one tissue microarray cohort of >650 patients, increasing NHERF1 and HER2 expression interacted to predict increased mortality (24). Our laboratory has demonstrated that in HER2-positive breast cancer cells, NHERF1 interacts with PMCA2 as part of a multiprotein signaling complex that also includes ezrin and HSP90, as well as HER2, EGFR, and HER3 (14, 15, 24). The formation of this complex is required to maintain activated HER2 at the cell surface, and loss of NHERF1 is associated with internalization and degradation of HER2, which, in turn, profoundly inhibits downstream HER2 signaling (24).

The splice variant of PMCA2 expressed by the mammary gland (PMCA2wb) contains an extended C-terminal domain ending in a canonical, PDZ recognition sequence (ETSL) shown to mediate its interaction with NHERF1 in CHO and MCF10A cells (24, 42, 43). Given the important interactions between PMCA2 and NHERF1 in HER2-positive breast cancer cells, we hypothesized that NHERF1 may be involved in the apical localization of PMCA2 in mammary epithelial cells. In this study, we demonstrate that, indeed, NHERF1 and PMCA2 colocalize in the apical plasma membrane in lactating mammary epithelial cells. Furthermore, we demonstrate that NHERF1 is important for the proper localization of PMCA2 and the maintenance of normal cell polarity and that it contributes to the prevention of early involution.

Materials and Methods

Mouse models

NHERF1 knockout (KO) mice were originally generated by Weinman and colleagues (44) and then backcrossed to C57BL/6J mice for 10 generations (45). Teat sealing was performed on lactating female mice on day 10 postpartum (46, 47). Vetbond (3M, St. Paul, MN; catalog no. 1469SB) adhesive was used to block the primary duct of the fourth inguinal mammary gland on the left side, after which mice were euthanized and mammary glands harvested at 2, 4, 8, and 24 hours after teat sealing. The contralateral right fourth inguinal mammary gland was harvested to serve as the unsealed control. Each teat sealing

experiment and time point was performed on three mice. All mouse experiments were reviewed and approved by the Yale University Institutional Animal Care and Use Committee.

Histology and immunohistochemistry

Whole mammary glands were fixed in 4% paraformaldehyde at 4°C for 12 hours. Antigen retrieval was accomplished by heating sections in 7 mM citrate, under pressure. Sections were incubated overnight at 4°C with primary antibodies. Primary antibodies include those against phospho-STAT3 (48) and phospho-STAT5 (49), from Cell Signaling Technology (Danvers, MA) and β-casein (50) from Santa Cruz Biotechnology (Dallas, TX). Staining was detected using Vector Elite ABC kits (Vector Laboratories, Burlingame, CA) and 3,3′-diaminobenzidine (Vector Laboratories).

The percentages of secretory alveoli were scored on hematoxylin and eosin (H&E)–stained sections for the presence or absence of suprabasal epithelial cells. In sections from three different wild-type (WT) or NHERF1KO mice, we examined 8 to 10 alveoli in different randomly selected high-power (×40) microscopic fields and scored a total of 50 alveoli for each mouse (150 total for each genotype). To determine the percentage of Stat3-positive cells we examined three sections for each genotype, one each from three separate mice. All cells in a randomly chosen ×10 field were counted and nuclei were scored as either STAT3 positive or negative.

Immunofluorescence

Paraffin-embedded tissue sections of mammary glands were cleared with Histo-Clear (National Diagnostics, Atlanta, GA) and graded alcohol using standard techniques (15, 24). Antigen retrieval was performed using 7 mM citrate buffer (pH 6.0) under pressure. Sections were incubated with primary antibody overnight at 4°C and with secondary antibody for 1 hour at room temperature. Coverslips were mounted using ProLong Gold antifade reagent with 4′,6-diamidino-2-phenylindole (Invitrogen). All images were obtained using a Zeiss 780 confocal microscope. Primary antibodies included those against NHERF1 (51, 52), PMCA2 (53), NHERF2 (54), and Na/K ATPase (55) from Santa Cruz Biotechnology; GATA3 (56) and β-catenin (57) from BD Pharmingen (San Jose, CA); α-smooth muscle actin (58) and lamp2 (59) from Abcam (Cambridge, UK); PMCA2 (60), cathepsin B (61), and wheat germ agglutinin/Alexa Fluor 555 conjugate (62) from Invitrogen (Grand Island, NY); and Ezrin (63), NHERF2 (64), phospho-STAT3 (48), phospho-STAT5 (49), cleaved caspase 3 (65), and ZO-3 (66) from Cell Signaling Technology (Danvers, MA). Npt2b antibody (67) was a gift from Dr. Jurg Biber at the University of Zurich.

Immunoblotting

Protein samples were prepared from tissues using standard methods (15, 24) and were subjected to SDS-PAGE and transferred to a nitrocellulose membrane by wet Western blot transfer (Bio-Rad Laboratories, Hercules, CA). The membrane was blocked in Tris-buffered saline with 1% Tween 20 (TBST) buffer containing 5% milk for 1 hour at room temperature. The blocked membranes were incubated overnight at 4°C with specific primary antibodies (Odyssey blocking buffer; catalog no. 927-40000). The membranes were washed three times with TBST buffer and then incubated with specific secondary antibodies provided by LI-COR Biosciences (Lincoln, NE) for 2 hours at room temperature. After three washes with TBST buffer, the membranes were analyzed using the Odyssey IR imaging system (LI-COR Biosciences). All immunoblot experiments were performed at least three times, and representative blots are shown in the figures.

RNA extraction and real-time RT-PCR

RNA was isolated using TRIzol (Invitrogen, Waltham, MA). Quantitative RT-PCR was performed with the SuperScript III Platinum one-step quantitative RT-PCR kit (Invitrogen) using a StepOnePlus real-time PCR system (Applied Biosystems, Waltham, MA) and the following TaqMan primer set: NHERF1, Mm00488865_m1; keratin 8, Mm04209403_g1; NHERF2; Mm00502650_m1. Mouse GAPD (Applied Biosystems; catalog no. 4351309) was used as a reference gene. Relative mRNA expression was determined using the StepOne software v2.2.2 (Applied Biosystems).

Proximity ligation assays

Proximity ligation assays (PLAs) were performed using the Duolink® assay kit (Sigma-Aldrich, St. Louis, MO). Paraffin-embedded tissue sections were cleared with Histo-Clear (National Diagnostics) and graded alcohol using standard techniques as above. Antigen retrieval was performed using 7 mM citrate buffer (pH 6.0) under pressure. Then, tissue sections were permeabilized with 0.1% Triton X-100 in PBS. Permeabilized sections were incubated with combinations of the following antibodies: rabbit anti-NHERF1 (51) or rabbit anti-NHERF2 (64) and mouse anti-PMCA2 (53). Antibodies for NHERF1 or NHERF2 were omitted for negative controls. PLA probes were then added and the assay was performed as per the manufacturer's instructions. Results are expressed as the absolute number of PLA dots per alveolus.

Milk calcium and protein analysis

Milk was diluted 1:100 in distilled water, and total milk calcium was measured using the colorimetric QuantiChrom calcium assay kit (BioAssay Systems, Hayward, CA). Protein concentrations were determined using the Bradford reagent (Bio-Rad Laboratories) with BSA standards, and calcium concentrations were normalized to milk protein concentrations (12, 68).

Statistical analysis

Statistical analyses were performed with Prism 7.0 (GraphPad Software, La Jolla, CA). Statistical significance was determined using an unpaired *t* test for comparisons between two groups and one-way ANOVA for groups of three or more.

Data availability

Most data generated or analyzed during this study are included in this published article or can be found in the microarray database in the "References and Notes" section (69). Some data presented in this paper are representative of multiple repeats not shown. Although not published in this study, these data are available from the corresponding author upon reasonable request.

Results

NHERF1 is expressed in mammary epithelial cells

We first examined the expression of NHERF1 mRNA in a microarray study of murine mammary glands during

pregnancy, lactation, and postweaning involution (12, 69). We also examined the expression of the closely related scaffolding molecule, NHERF2, which has also been shown to interact with PMCA2, and compared both to the previously defined levels of PMCA2 mRNA (12, 43). PMCA2 mRNA expression is upregulated at the transition between pregnancy and lactation and then is promptly downregulated at weaning (12, 68, 70) (Fig. 1A). NHERF1 mRNA levels followed the general pattern of PMCA2 expression, but they increased somewhat earlier during the latter half of pregnancy and peaked during lactation. Similar to PMCA2, NHERF1 mRNA levels decreased rapidly during early involution, but they did not return entirely to baseline until the completion of involution. NHERF2 mRNA levels also increased slightly during lactation, but NHERF1 expression appeared to be higher than NHERF2 expression in the mammary gland at all stages, and NHERF1 expression increased to a much greater extent than did NHERF1 during pregnancy and lactation. Therefore, we chose to concentrate further studies on NHERF1. To independently validate the changes in NHERF1 expression during lactation, we measured its mRNA levels in virgin and lactating mammary glands by quantitative PCR (qPCR). Because the epithelial content of the mammary gland is quite different in virgin as compared with lactating mammary glands, and because NHERF1 is expressed in luminal epithelial cells (see below), we normalized NHERF1 mRNA levels to K18 mRNA, which is expressed in luminal epithelial cells. As shown in Fig. 1B, normalized NHERF1 mRNA levels were almost sixfold higher during lactation as compared with virgin glands, validating the changes noted in the microarray.

We examined NHERF1 protein levels and localization by performing immunofluorescence staining in mammary ducts from 3-week-old virgin mice and in

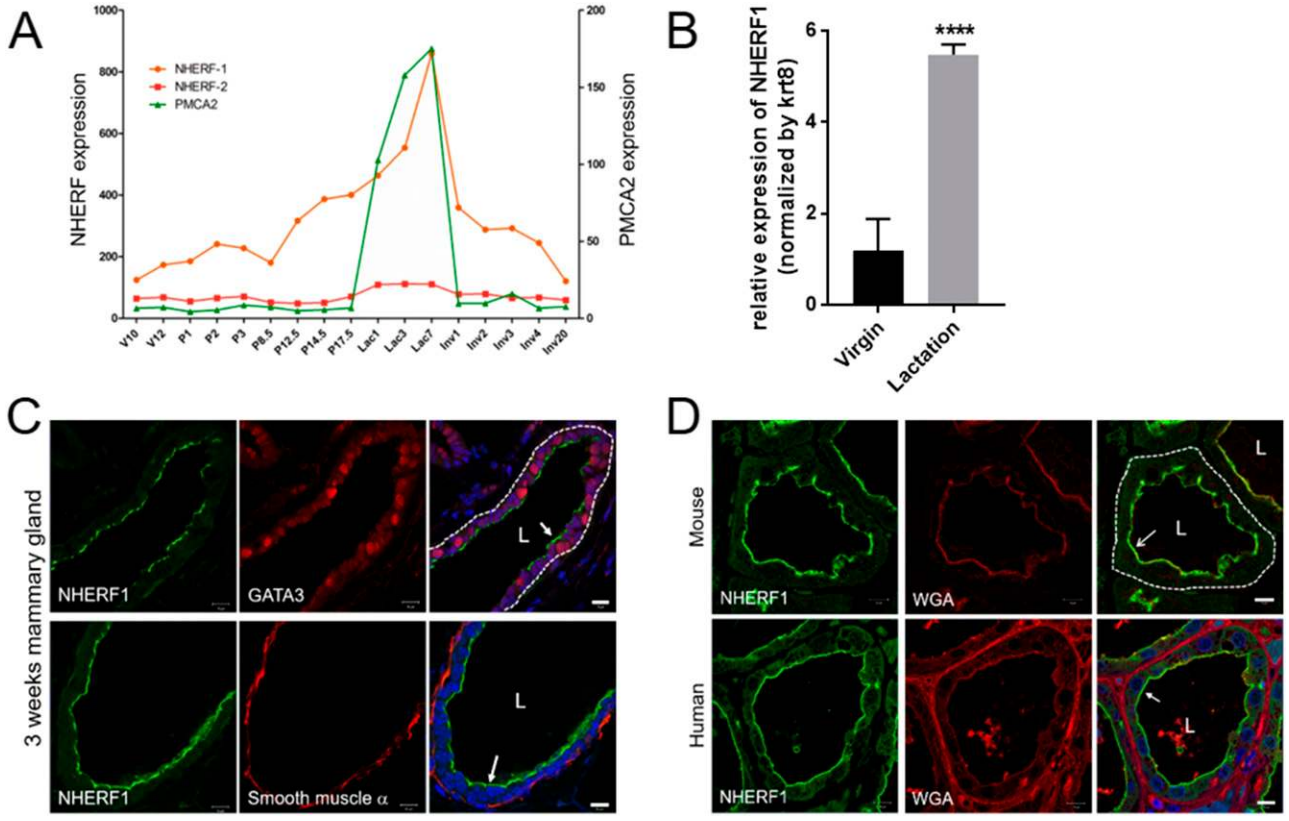

Figure 1. NHERF1 expression in mammary epithelial cells. (A) Expression profiles of NHERF1 (orange line), NHERF2 (red line), and PMCA2 (green line) mRNAs during mammary development in mice. Data were extracted from a microarray study profiling mammary glands from 10- and 12-wk-old virgins (V), days 1, 2, 3, 8.5, 14.5, and 17.5 of pregnancy, days 1, 3, and 7 of lactation (Lac), and days 1, 2, 3, 4, and 20 of involution (Inv). (B) NHERF1 mRNA expression in mammary glands from virgin and lactating mice as assessed by qPCR. NHERF1 expression was normalized to keratin 18 expression to correct for changes in epithelial cell content in virgin vs lactating mammary glands. Bars show mean ± SEM of three repeats. $****P < 0.0001$. (C) Typical immunofluorescence staining for NHERF1 (green) and the luminal cell marker GATA3 (red, top row) or the myoepithelial cell marker smooth muscle α-actin (red, bottom row) in virgin mammary ducts. The last panels in each row show merged staining with 4′,6-diamidino-2-phenylindole (blue) to mark nuclei. The white dotted line delineates the basement membrane, L denotes the lumen, and white arrows point to the apical surface. Scale bars, 10 μm. (D) Immunofluorescence staining for NHERF1, PMCA2, and the luminal surface marker WGA in lactating mammary glands. Top row shows NHERF1 (green) and WGA staining (red) and colocalization in mouse mammary glands. Bottom row shows NHERF1 (green) and WGA staining (red) and colocalization in human mammary glands. Dotted lines show basement membrane, L denotes the alveolar lumen, and white arrows point toward apical membrane staining for NHERF1. Scale bars, 10 μm. WGA, wheat germ agglutinin.

mammary alveoli from day 12 of lactation. In the virgin gland, NHERF1 expression was located at the apical surface of luminal epithelial cells, identified by costaining for GATA3, a transcription factor found in luminal epithelial cells but not in myoepithelial cells (Fig. 1C) (71, 72). We did not detect NHERF1 immunofluorescence in myoepithelial cells, which were identified by immunostaining for α-smooth muscle cell actin (Fig. 1C) (71, 73). NHERF1 immunostaining was more prominent in lactating mammary glands (Fig. 1D) and was, again, located at the luminal surface as indicated by its colocalization with the apical marker wheat germ agglutinin (WGA) (74). We also performed immunofluorescence staining of lactating human breast samples and, as in mice, found prominent NHERF1 expression at the apical surface of alveolar epithelial cells (Fig. 1D).

NHERF1 and PMCA2 interact in lactating mammary epithelial cells

We had previously documented direct interactions between NHERF1 and PMCA2 in cell lines (24), and we next examined whether these molecules might also interact in lactating mammary epithelial cells *in vivo*. We costained for PMCA2 and NHERF1 in mouse mammary glands on day 10 of lactation. As expected, both NHERF1 and PMCA2 were expressed at the apical plasma membrane of alveolar epithelial cells (Fig. 2A and 2B), and they colocalized as illustrated by the yellow immunofluorescence shown in Fig. 2C. Although colocalization is consistent with their interaction, it is not definitive evidence that PMCA2 and NHERF1 directly interact *in situ*. Therefore, we also performed PLAs using primary antibodies against PMCA2 and NHERF1 and secondary antibodies labeled with oligonucleotides that can be ligated, amplified, and visualized with incorporated fluorescent PLA probes when the two proteins are in close proximity (<30 to 40 nM apart) (14, 75). As shown in Fig. 2E and 2F, a PLA signal could be detected over mammary epithelial cells in lactating glands, demonstrating close interactions between these two proteins. As a control for nonspecific interactions, when the NHERF1 antibody was excluded, no such signal could be detected (Fig. 2D). Taken together, co-immunofluorescence and PLA assay results are consistent with interactions between PMCA2 and NHERF1 during lactation in normal mammary epithelial cells *in vivo*.

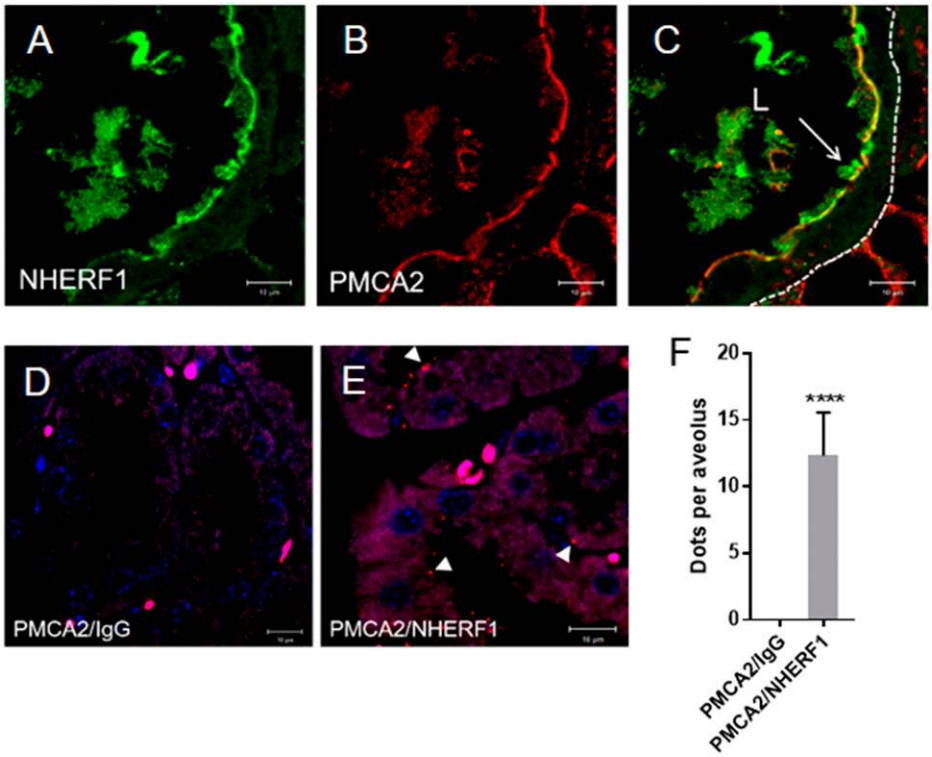

Figure 2. Interactions between NHERF1 and PMCA2. (A–C) Typical coimmunofluorescence staining for (A) NHERF1 (green) and (B) PMCA2 (red) in mammary glands at day 10 of lactation; (C) represents the merge of (A) and (B). Dotted line in (C) traces the alveolus basement membrane, L represents the lumen, and the white arrow points toward costaining for NHERF1 and PMCA2 at the apical membrane. (D and E) Representative images for PLA assay for PMCA2 antibody and control IgG in (D) and PMCA2 and NHERF1 antibodies in (E). White arrowheads in (E) point to fluorescent dots representing close interactions between PMCA2 and NHERF1. (F) Quantitation of PLA signals for PMCA2 antibody and control IgG in (D) and PMCA2 and NHERF1 antibodies. Bars represent the mean number of fluorescent signals per alveolus, and error bars represent SEM of two mammary glands analyzed. $****P < 0.0001$. Scale bars in panels (A)–(E), 10 μm.

NHERF1 expression decreases in response to milk stasis

NHERF1 mRNA levels decline rapidly (within 24 hours) during early involution (Fig. 1A), suggesting that downregulation of NHERF1 might be triggered by milk stasis. We confirmed this observation by examining NHERF1 mRNA and protein expression using the teat-sealing paradigm of early involution (46, 47). These experiments were done in an otherwise normal lactating mouse by plugging one of the fourth (inguinal) pair of teats, which induces milk stasis and triggers the first phase of involution specifically in that gland without affecting the other glands or changing circulating hormones. As can be seen, NHERF1 mRNA levels decreased between 4 and 24 hours after teat sealing as compared with levels noted in the contralateral gland, which was suckled normally (Fig. 3A). Interestingly, NHERF1 protein levels, as assessed by immunoblot, were significantly reduced by 2 hours after teat sealing and were essentially absent by 24 hours (Fig. 3B). This time course of reduced NHERF1 protein expression was mirrored by the results of immunofluorescence for NHERF1. Figure 3C demonstrates dramatic reductions in the intensity of NHERF1 immunostaining at 4 hours and 24 hours after teat sealing. These data suggest that NHERF1 protein levels are promptly reduced after weaning in response to the local effects of milk stasis rather than changes in systemic hormones. Additionally, our data suggest that protein levels are reduced prior to mRNA levels, implying active degradation of NHERF1 in response to milk stasis.

Loss of NHERF1 alters apical–basal polarity and PMCA2 localization

We next studied how loss of NHERF1 expression affects the mammary gland in lactating NHERF1KO mice (44). As expected, we could no longer detect NHERF1 immunofluorescence in mammary epithelial cells from NHERF1KO mice euthanized on day 10 of lactation (Fig. 4A). Immunoblot analysis also confirmed the loss of NHERF1 in lactating mammary glands (Fig. 4B).

Morales *et al.* (38) suggested that loss of NHERF1 caused an impairment of secretory differentiation of mammary epithelial cells and a reduction in alveolar mass during lactation due to disruption of normal prolactin–Stat5 signaling. However, we found normal alveolar mass and architecture in NHERF1KO glands as compared with WT controls (Fig. 4C). Additionally, there were no differences in the pattern or intensity of staining for nuclear pStat5 or β-casein in NHERF1KO epithelial cells as compared with WT epithelial cells, suggesting that secretory alveolar differentiation was intact (Fig. 4D and 4E). However, upon closer examination of the alveolar cells, several abnormalities were apparent. First, as shown in Fig. 4C and 4F, some secretory epithelial cells in the NHERF1KO gland appeared taller, more variable in shape, and, in many places, piled on top of each other, creating an abnormally multilayered secretory epithelium. These changes did not occur in all cells, but 51% ± 2.1% of NHERF1KO alveoli contained abnormally appearing suprabasal cells, whereas only 8.7% ± 1.3% of WT alveoli contained any suprabasal epithelial cells (P = 0.0002, 50 alveoli

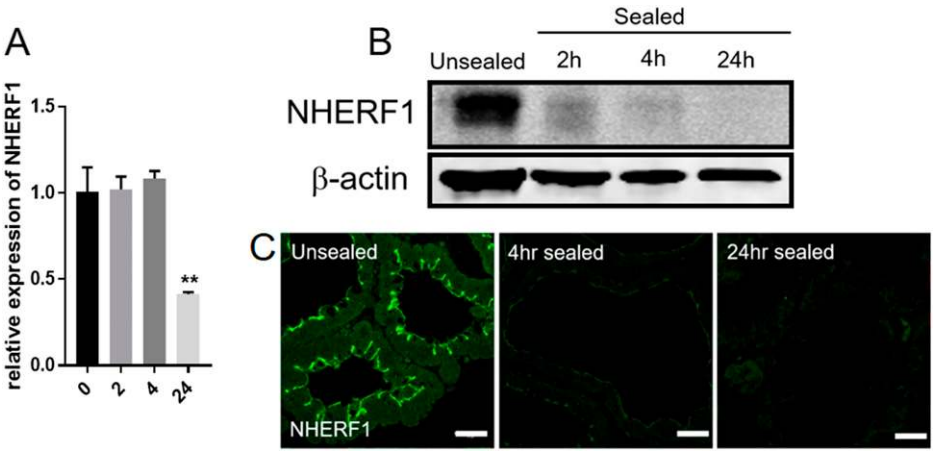

Figure 3. NHERF1 is reduced in response to milk stasis. (A) NHERF1 mRNA expression at 2, 4, and 24 h after teat sealing. Bars represent the mean ± SEM of levels compared with time 0 (unsealed glands) as measured by qPCR. $^{**}P < 0.01$. Assay was repeated on three different mammary glands for each point. (B) Representative immunoblot showing reductions in NHERF1 protein levels from mammary glands harvested 2, 4, or 24 h after teat sealing on day 10 of lactation. The unsealed gland represents the level of NHERF1 on day 10 of lactation in contralateral unsealed glands. (C) Representative immunofluorescence for NHERF1 (green) at 4 and 24 h after teat sealing at day 10 of lactation. Scale bar, 10 μm.

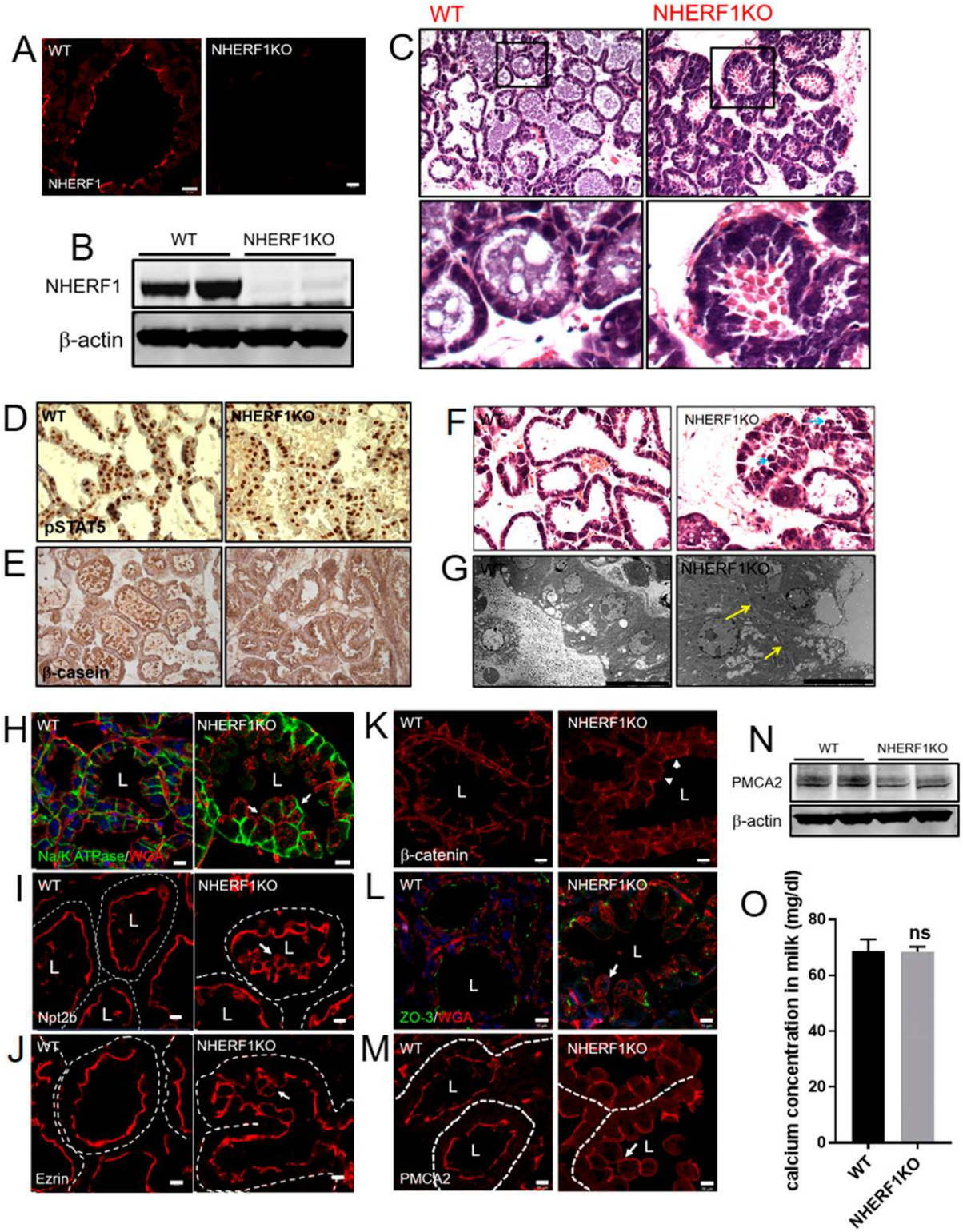

Figure 4. Loss of NHERF1 alters PMCA2 localization and epithelial cell polarity. (A) Immunofluorescence staining for NHERF1 in WT or NHERF1KO mammary glands on day 10 of lactation. (B) Immunoblot showing NHERF1 levels from WT or NHERF1KO mice. (C) H&E-stained histology of WT and NHERF1KO mammary glands during lactation. Boxed areas on top row are magnified in bottom row. (D and E) Immunohistochemical staining for (D) phospho-STAT5 and (E) β-casein in WT or NHERF1KO mammary glands on day 10 of lactation. (F) H&E-stained histology of WT and NHERF1KO mammary glands during lactation showing multilayered luminal epithelial cells (yellow arrows) in NHERF1KO mammary glands. (G) Transmission electron micrographs of lactating mammary glands from WT (left) and NHERF1KO (right) mice. Yellow arrows point to abnormal superbasal epithelial cells in the NHERF1KO glands. (H–J) Immunofluorescence staining for (H) Na/K ATPase (green) and WGA (red), (I) Npt2b, and (J) ezrin in WT or NHERF1KO mammary glands on day 10 of lactation. L represents lumens, and dotted white lines outline the alveolar basement membrane. White arrows in (H) demonstrate apical expression of Na/K ATPase in NHERF1KO glands. White arrows in (I) and (J) demonstrate cells with basolateral extension of Npt2b and ezrin expression. (K and L) Immunostaining for (K)

assessed in each of three glands of each genotype). Upon transmission electron microscopy, lactating WT glands demonstrated a single layer of polarized, secretory epithelial cells with basally located nuclei and apical, lipid-filled granules (Fig. 4G). In contrast, NHERF1KO glands demonstrated multiple, superbasal epithelial cells, which had variable shapes and contained abnormally large lipid droplets in the apical region. Second, immunostaining for apical and basolateral markers demonstrated that these cells had disturbed polarity (Fig. 4H–4L). In control glands, there was no apical expression of the basolateral marker Na/K ATPase. However, in NHERF1KO glands, Na/K ATPase was distributed around the entire perimeter of many cells (Fig. 4H). Similarly, in WT glands, the apical markers Npt2b and ezrin were limited to luminal surfaces, but in NHERF1KO glands, cells adjacent to the lumen of the alveoli showed expression of ezrin and Npt2b around their entire perimeter (Fig. 4I and 4J). Loss of NHERF1 also disrupted components of the junctional complexes separating the apical from basolateral surfaces of some epithelial cells. Primarily in the abnormal suprabasal secretory alveolar cells, there was apical expression of β-catenin and loss of ZO-3 expression (Fig. 4K and 4L). Finally, overall PMCA2 levels were reduced on Western analysis and, consistent with the extension of ezrin and NPT2b into the basolateral surface of the multilayered luminal cells, immunofluorescence for PMCA2 was also found throughout the membrane of these cells (Fig. 4M and 4N). Despite these abnormalities in PMCA2 expression and localization, overall milk calcium levels were not changed in milk collected from NHERF1KO dams (Fig. 4O).

Previous studies in breast cancer cells demonstrated a much greater reduction in total PMCA2 protein levels upon knocking down expression of NHERF1 (24). Therefore, we were surprised that PMCA2 levels were not more severely reduced in lactating NHERF1KO glands. We hypothesized that, in the absence of NHERF1, NHERF2 might be able to stabilize PMCA2 at the plasma membrane even though PMCA2 was no longer solely at the apical surface. As shown in Fig. 5A and 5B, total NHERF2 protein and mRNA levels were unchanged in lactating NHERF1KO mammary glands. In WT glands, NHERF2, similar to NHERF1, was restricted to the apical surface of the secretory epithelial cells and colocalized with PMCA2 (Fig. 5C). Additionally, proximity ligation assays suggested that NHERF2 interacted with PMCA2 in WT mammary glands (Fig. 5D and 5E). In NHERF1KO glands, NHERF2 and PMCA2 still colocalized by immunofluorescence staining, but both were now found throughout the membrane of the multilayered luminal epithelial cells, suggesting that NHERF2 may help maintain PMCA2 at the membrane, if not solely at the apical surface, in these cells (Fig. 5C). Interestingly, similar to NHERF1, NHERF2 expression is also reduced by milk stasis at both the mRNA and protein levels (Fig. 5F and 5G).

Loss of NHERF1 activates early involution pathways in a subset of epithelial cells

In lactating NHERF1KO mice, we noted rare, abnormally appearing cells that stained for cleaved caspase-3 and that were shed into the lumen of the glands (Fig. 6A and 6B). These cells were not present in control glands and, although many fewer in number, were reminiscent of mammary epithelial cells that are shed into the lumen of early involuting glands as well as those noted in lactating, PMCA2-null mammary glands (6, 7, 68). Therefore, we asked whether loss of NHERF1 expression activated premature involution in lactating mammary glands by examining activation of the Stat3–LMP cell death pathway. As shown in Fig. 6C and 6D, 9.3% $\pm$ 1.0% of mammary epithelial cells in the NHERF1KO glands from mid-lactation demonstrated activation of Stat3 as shown by nuclear staining for phospho-Stat3. Interestingly, many of the phospho-Stat3-positive cells remained positive for phospho-Stat5, which is similar to coexpression of phospho-Stat3 and phospho-Stat5 in early involution (Fig. 6E). Consistent with the activation of Stat3, NHERF1KO cells showed upregulation of cathepsin B and LAMP2 expression (Fig. 6F), hallmarks of the lysosomal membrane permeabilization cell death pathway that becomes activated during early mammary gland involution (6, 7). Thus, during lactation, loss of NHERF1 expression caused premature activation of a milk stasis–related involution/LMP program in patchy areas of the mammary glands. Although this occurred in a minority of the cells, normally this pathway is silent during lactation and is activated only in response to milk stasis after weaning (3, 4).

Discussion

In this study, we demonstrate that NHERF1 expression is increased in the mammary gland during lactation and is found at the apical membrane of secretory, luminal

Figure 4. (Continued). β-catenin and (L) ZO-3 (green) staining in WT or NHERF1KO mammary glands on day 10 of lactation. Arrows point to apical expression of β-catenin and loss of ZO-3 expression in the abnormal superbasal luminal epithelial cells in NHERF1KO glands. (M) PMCA2 expression in WT or NHERF1KO mammary glands on day 10 of lactation. White dotted line delineates the alveolar basement membrane. Arrows point to basolateral extension of PMCA2 expression in NHERF1KO mammary epithelial cells. (N) Representative immunoblot showing reduction in overall PMCA2 expression in NHERF1KO vs WT mammary glands harvested on day 10 of lactation. (O) Calcium concentrations in milk (normalized to protein content) collected from WT or NHERF1KO mice on day 10 of lactation. Scale bars, 10 μm. Histology and immunohistochemistry images were taken at $\times$400 magnification. Bars represent mean $\pm$ SEM of three measurements.

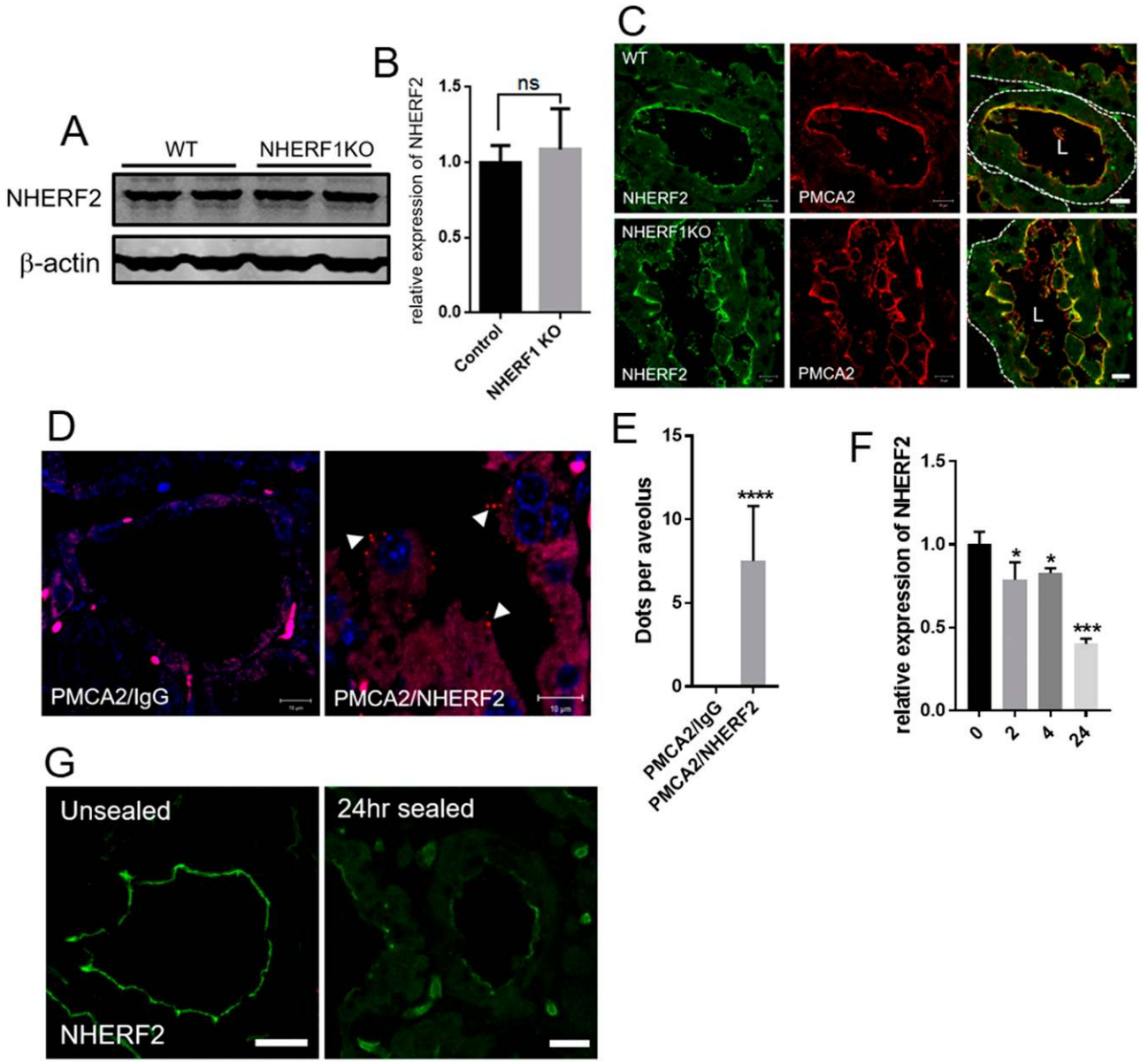

Figure 5. NHERF2 expression in NHERF1KO mammary glands. (A) Immunoblot showing NHERF2 levels from WT or NHERF1KO mice. (B) Quantitative RT-PCR analysis of NHERF2 expression from WT or NHERF1KO mice. Bars represent mean ± SEM of three mammary glands. Results are shown as change relative to WT glands. (C) Immunofluorescence staining for NHERF2 (green) and PMCA2 (red) in mammary glands from lactating WT (top row) or NHERF1KO (bottom row) mice. Panels on the right show costaining for NHERF2 and PMCA2. Dotted lines show alveolar basement membranes, and L denotes the alveolar lumen. Scale bars, 10 μm. (D) Representative images for PLA assay of lactating WT mammary gland for PMCA2 antibody and control IgG on left and PMCA2 and NHERF2 antibodies on right. White arrowheads in right panel point to fluorescent dots representing close interactions between PMCA2 and NHERF2. Scale bars, 10 μm. (E) Bar graph represents quantitation of PLA signals for PMCA2 antibody and control IgG as well as for PMCA2 and NHERF1 antibodies. Bars represent the mean number of fluorescent signals per alveolus, and error bars represent SEM of two repeats. $^{****}P < 0.0001$. (F) Reduction in NHERF2 mRNA levels in response to teat sealing as determined by qPCR. Bars represent the mean and SEM of three glands harvested at 2, 4, or 24 h after teat sealing. Time 0 represents the baseline levels in the contralateral unsealed glands, and data are presented as the proportion relative to the unsealed mean. $^{*}P < 0.05$; $^{***}P < 0.001$. (G) Representative immunofluorescence for NHERF2 (green) at baseline (unsealed) and 24 h after teat sealing at day 10 of lactation. Scale bars, 10 μm.

epithelial cells in both mice and humans. We also found that the expression of the closely related scaffolding molecule, NHERF2, is upregulated during lactation and is also found at the apical surface. However, NHERF1 appears to be more prominently expressed than NHERF2 in the lactating breast. NHERF1 colocalizes and interacts with PMCA2 at the luminal surface of lactating alveoli in the mammary gland, and NHERF1 contributes to the maintenance of PMCA2 within the apical membrane domain of secretory epithelial cells. In the absence of NHERF1, overall PMCA2 expression is reduced and its pattern of expression is altered and extends to the basolateral aspects of many mammary epithelial cells. Finally, we show that loss of NHERF1

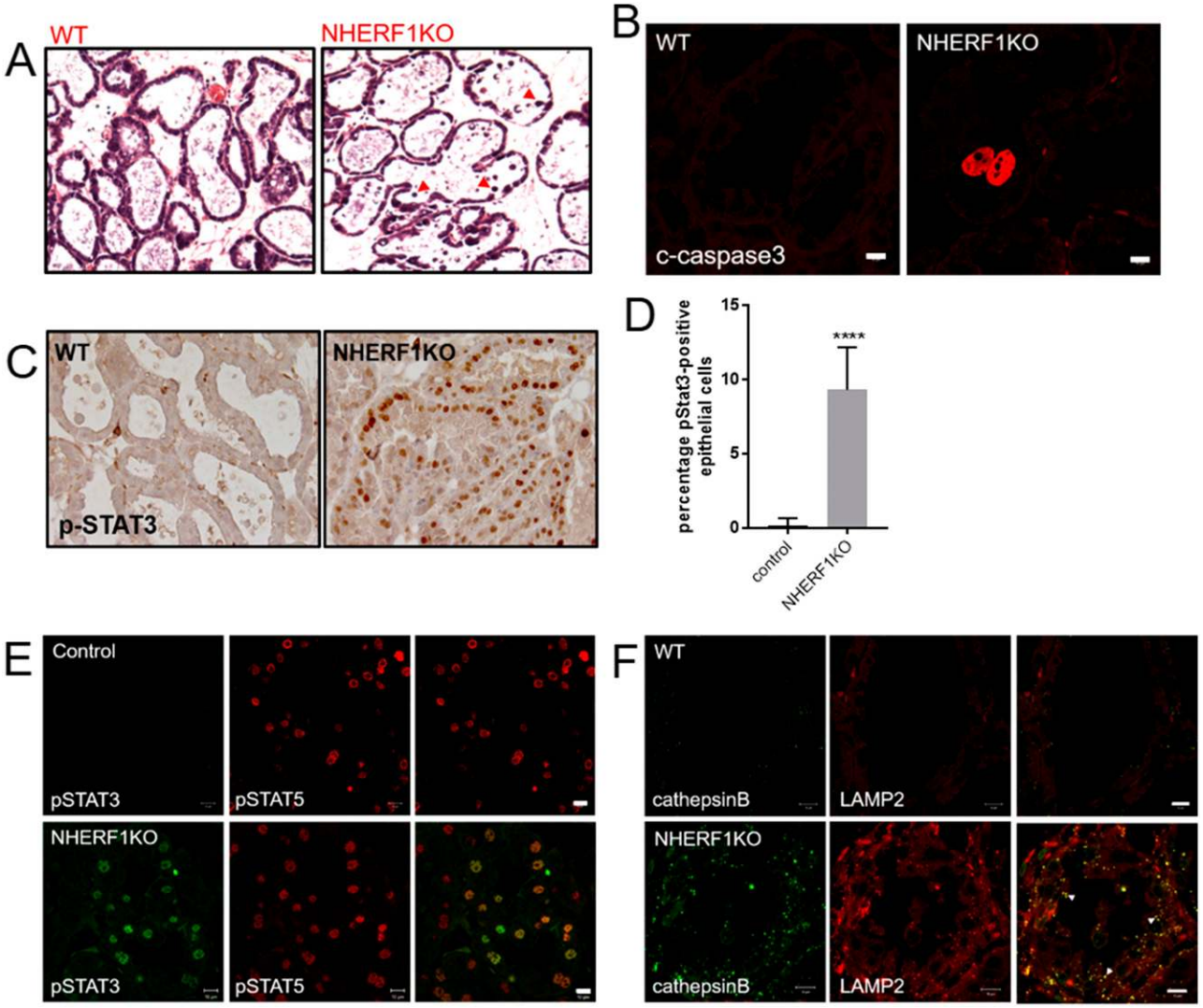

Figure 6. Loss of NHERF1 activates early involution pathways during lactation. (A) H&E-stained histology of WT and NHERF1KO mammary glands during lactation. Red arrows point to epithelial cells shed into the alveolar lumen (×400 magnification). (B) Immunofluorescence for cleaved caspase-3 in lactating WT or NHERF1KO mammary glands. Scale bars, 10 μm. (C) Immunohistochemical staining for pSTAT3 in WT (left) or NHERF1KO (right) mammary glands on day 10 of lactation (×400 magnification). (D) Percentage of epithelial cells positive for nuclear phospho-Stat3 immunostaining (3610 epithelial cells were counted for WT mice and 5070 cells were counted for NHERF1KO mice). ****$P <$ 0.0001. (E) Immunofluorescence costaining for phospho-Stat3 (left), phospho-Stat5 (middle), or the merged images (right) in lactating WT (top row) or NHERF1KO (bottom row) mice. (F) Typical immunofluorescence costaining for cathepsin B (left), LAMP2 (middle), or the merged images (right) in lactating WT (top row) or NHERF1KO (bottom row) mice. White arrowheads point to colocalization of cathepsin B and LAMP2 in epithelial cells in NHERF1KO mammary glands. Scale bars, 10 μm.

promotes premature activation of STAT3 in 9% of mammary epithelial cells, which is associated with patchy induction of early involution pathways, cell shedding, and cell death during lactation. These findings are consistent with the participation of NHERF1 in maintaining normal mammary epithelial cell organization and its contribution to cell survival during lactation.

Mammary epithelial cells express the PMCA2w/b splice variant, which contains a C-terminal PDZ interaction motif and traffics to the apical membrane (10, 12, 43). During lactation, PMCA2 transports calcium into milk and prevents calcium-induced death of secretory epithelial cells (11–13, 68, 70). The presence of a C-terminal PDZ binding motif within PMCA2 suggested that NHERF1 and/or NHERF2 might interact with PMCA2 and influence its membrane localization. Prior work showed that PMCA2 interacted with NHERF2 in MDCK and COS-1 cells and that binding with NHERF2 stabilized PMCA2 at the apical membrane, preventing its lateral mobility and internalization (42, 43). However, in CHO cells and MCF10A cells, we previously found that PMCA2 interacts equally well with NHERF1 and NHERF2 (24). PMCA2 likely interacts with both NHERF1 and NHERF2 in mammary epithelial cells *in vivo* because mammary gland PMCA2 levels were only moderately reduced and milk calcium levels were unchanged in

lactating NHERF1KO mice. Furthermore, NHERF1 and NHERF2 both interacted closely with PMCA2, as determined by proximity ligation assays, and NHERF2 continued to colocalize with PMCA2 in NHERF1KO mammary epithelial cells even though both were abnormally distributed to the basolateral surface of some cells. These findings suggest that NHERF1 is required for proper apical localization of PMCA2 but that both NHERF1 and NHERF2 may cooperate to maintain PMCA2 at the cell membrane, similar to what has been described for NHE3 in renal and intestinal epithelial cells (76, 77). Testing this hypothesis will require future examination of PMCA2 localization and expression in NHERF2KO mammary glands as well as NHERF1/NHERF2 compound heterozygous and double-KO mice.

It is unclear whether the abnormal basolateral localization of PMCA2 in NHERF1KO epithelial cells is the consequence of loss of specific anchoring of PMCA2 via PDZ interactions with NHERF1 or whether it is due, more nonspecifically, to the loss of apical–basal polarization of these cells. The alveolar cellular architecture in lactating NHERF1KO mammary glands is abnormal, containing regions of multilayered secretory epithelial cells in half of all alveoli. These cells appeared abnormally shaped and failed to properly restrict PMCA2, NPT2b, and ezrin to the apical membrane as well as Na/K ATPase to the basolateral membrane. These results are consistent with prior studies demonstrating the importance of NHERF1 in the generation and maintenance of apical membrane structure and cell polarity in a variety of epithelial cells (21, 22, 25). However, we did not find complete disruption of apical expression of PMCA2, NPT2b, or ezrin, and many cells had relatively normal expression of ZO-3 and membrane-associated β-catenin. We do not understand the heterogeneity of the phenotype in these cells, as loss of NHERF1 appears to be uniform in mammary epithelial cells in NHERF1KO mice (Fig. 4A and 4B). This heterogeneity may result from the preservation of NHERF2 in these cells, which has also been shown to participate in apical localization of PMCA2 and NHE3 in other epithelial cell types (43, 76, 77). The most abnormal expression of apical and basolateral markers was in cells that appeared to reside on top of more normal-appearing luminal cells. It is likely that these abnormally polarized cells are ultimately shed into the lumen and die, as they did not collect to fill the lumens.

Loss of PMCA2 causes widespread, premature involution during lactation associated with elevations in intracellular calcium in mammary epithelial cells (68). We now show that loss of NHERF1 is also associated with premature activation of early involution pathways, although in a patchy distribution of $<10\%$ of secretory epithelial cells, many fewer cells than were affected by loss of PMCA2. The affected cells in NHERF1KO glands showed upregulation of phospho-Stat3, cathepsin K, and Lamp2 expression, as well as shedding of caspase-3–positive epithelial cells into the alveolar lumen. These findings are reminiscent of activation of the Stat3-dependent LMP pathway of cell death caused by milk stasis, and, interestingly, milk stasis was sufficient to induce the rapid downregulation of NHERF1 within 2 to 4 hours of experimental teat sealing (6, 7). These results suggest that the decrease of NHERF1 expression after weaning may contribute to the initiation of LMP-mediated cell death during the first phase of mammary gland involution. In breast cancer cells, loss of NHERF1 leads to a dramatic downregulation of PMCA2 expression, as well as intracellular calcium-mediated cell death (24). However, NHERF1 may scaffold many different membrane receptors and ion pumps, and it is not clear whether the LMP-like changes that we observed in NHERF1KO glands are due to alterations in PMCA2 levels and/or localization, or to disruptions in some other survival signaling pathway (31, 32). As discussed previously, the generation of NHERF1/NHERF2 compound heterozygous and double-KO mice may help to resolve whether NHERF2 is partially substituting for NHERF1 by supporting PMCA2 levels. If this is the case, we would expect that loss of both NHERF1 and NHERF2 might cause more widespread cell death during lactation, better approximating the widespread premature involution caused by loss of PMCA2 (68).

Morales *et al.* (38) reported that NHERF1 was required for the basolateral localization and function of the prolactin receptor. However, in our studies, NHERF1KO mice were able to feed their litters, mammary epithelial cells had normal nuclear pStat5 staining, and alveolar cell mass and the expression of markers of secretory differentiation were normal. All of these findings are inconsistent with a loss of prolactin signaling, although we did not directly assay prolactin receptor or Jak2 expression and/or phosphorylation, given that phospho-Stat5 levels were normal (78–81). Additionally, we found clear and specific immunofluorescence staining for NHERF1 at the apical, not basolateral, surface of mammary epithelial cells from lactating mice and humans, findings consistent with other studies of its location in a variety of secretory epithelia as well as with prior reports demonstrating apical NHERF1 expression in normal breast cells (21–23, 25, 34, 41, 44, 82). It is not clear why our findings differ from the previous report.

In summary, our studies support the participation of NHERF1 in maintaining the proper apical localization of PMCA2 in lactating mammary glands *in vivo*. Loss of NHERF1 results in abnormal cell morphology and alterations in apical–basal polarity in luminal epithelial

cells in the lactating gland. Loss of NHERF1 expression also causes activation of Stat3 in almost 10% of epithelial cells and the shedding of dying cells into the alveolar lumen. This is associated with the upregulation of lysosomal markers, consistent with activation of the LMP pathway of cell death characteristic of early mammary gland involution. We conclude that NHERF1 contributes to the maintenance of proper epithelial cell polarity and the proper pattern of PMCA2 expression, which, we hypothesize, helps to suppress Stat3 activation and prevent premature mammary gland involution.

Acknowledgments

The authors thank Dr. Virginia Borges (Young Women's Breast Cancer Translational Program, University of Colorado Hospital) for assistance with human tissue acquisition.

Financial Support: This work was supported by National Institutes of Health Grants HD076248 (to J.J.W.), CA169175 (to P.S.), and DK105811 (to P.A.F.).

Correspondence: John J. Wysolmerski, MD, Section of Endocrinology and Metabolism, Department of Internal Medicine, TAC S123a, Yale University School of Medicine, 333 Cedar Street, FMT 102, Box 208020, New Haven, Connecticut 06520. E-mail: john.wysolmerski@yale.edu.

Disclosure Summary: The authors have nothing to disclose.

References and Notes

1. Guo Q, Betts C, Pennock N, Mitchell E, Schedin P. Mammary gland involution provides a unique model to study the TGF-β cancer paradox. *J Clin Med*. 2017;**6**(1):E10.
2. Hughes K, Watson CJ. The multifaceted role of STAT3 in mammary gland involution and breast cancer. *Int J Mol Sci*. 2018;**19**(6):E1695.
3. Jena MK, Jaswal S, Kumar S, Mohanty AK. Molecular mechanism of mammary gland involution: an update. *Dev Biol*. 2019;**445**(2):145–155.
4. Watson CJ. Involution: apoptosis and tissue remodelling that convert the mammary gland from milk factory to a quiescent organ. *Breast Cancer Res*. 2006;**8**(2):203.
5. Lund LR, Rømer J, Thomasset N, Solberg H, Pyke C, Bissell MJ, Danø K, Werb Z. Two distinct phases of apoptosis in mammary gland involution: proteinase-independent and -dependent pathways. *Development*. 1996;**122**(1):181–193.
6. Kreuzaler PA, Staniszewska AD, Li W, Omidvar N, Kedjouar B, Turkson J, Poli V, Flavell RA, Clarkson RW, Watson CJ. Stat3 controls lysosomal-mediated cell death in vivo. *Nat Cell Biol*. 2011;**13**(3):303–309.
7. Sargeant TJ, Lloyd-Lewis B, Resemann HK, Ramos-Montoya A, Skepper J, Watson CJ. Stat3 controls cell death during mammary gland involution by regulating uptake of milk fat globules and lysosomal membrane permeabilization. *Nat Cell Biol*. 2014;**16**(11):1057–1068.
8. Brini M, Carafoli E. Calcium pumps in health and disease. *Physiol Rev*. 2009;**89**(4):1341–1378.
9. Strehler EE. Plasma membrane calcium ATPases as novel candidates for therapeutic agent development. *J Pharm Pharm Sci*. 2013;**16**(2):190–206.
10. Strehler EE, Zacharias DA. Role of alternative splicing in generating isoform diversity among plasma membrane calcium pumps. *Physiol Rev*. 2001;**81**(1):21–50.
11. Reinhardt TA, Lippolis JD, Shull GE, Horst RL. Null mutation in the gene encoding plasma membrane Ca^{2+}-ATPase isoform 2 impairs calcium transport into milk. *J Biol Chem*. 2004;**279**(41):42369–42373.
12. VanHouten JN, Neville MC, Wysolmerski JJ. The calcium-sensing receptor regulates plasma membrane calcium adenosine triphosphatase isoform 2 activity in mammary epithelial cells: a mechanism for calcium-regulated calcium transport into milk. *Endocrinology*. 2007;**148**(12):5943–5954.
13. VanHouten JN, Wysolmerski JJ. Transcellular calcium transport in mammary epithelial cells. *J Mammary Gland Biol Neoplasia*. 2007;**12**(4):223–235.
14. Jeong J, Choi J, Kim W, Dann P, Takyar F, Gefter JV, Friedman PA, Wysolmerski JJ. Inhibition of ezrin causes PKCα-mediated internalization of erbb2/HER2 tyrosine kinase in breast cancer cells. *J Biol Chem*. 2019;**294**(3):887–901.
15. Jeong J, VanHouten JN, Dann P, Kim W, Sullivan C, Yu H, Liotta L, Espina V, Stern DF, Friedman PA, Wysolmerski JJ. PMCA2 regulates HER2 protein kinase localization and signaling and promotes HER2-mediated breast cancer. *Proc Natl Acad Sci USA*. 2016;**113**(3):E282–E290.
16. Ardura JA, Friedman PA. Regulation of G protein-coupled receptor function by Na^+/H^+ exchange regulatory factors. *Pharmacol Rev*. 2011;**63**(4):882–900.
17. Bretscher A, Chambers D, Nguyen R, Reczek D. ERM-Merlin and EBP50 protein families in plasma membrane organization and function. *Annu Rev Cell Dev Biol*. 2000;**16**(1):113–143.
18. Brône B, Eggermont J. PDZ proteins retain and regulate membrane transporters in polarized epithelial cell membranes. *Am J Physiol Cell Physiol*. 2005;**288**(1):C20–C29.
19. Voltz JW, Weinman EJ, Shenolikar S. Expanding the role of NHERF, a PDZ-domain containing protein adapter, to growth regulation. *Oncogene*. 2001;**20**(44):6309–6314.
20. Weinman EJ, Hall RA, Friedman PA, Liu-Chen LY, Shenolikar S. The association of NHERF adaptor proteins with G protein-coupled receptors and receptor tyrosine kinases. *Annu Rev Physiol*. 2006;**68**(1):491–505.
21. Bryant DM, Roignot J, Datta A, Overeem AW, Kim M, Yu W, Peng X, Eastburn DJ, Ewald AJ, Werb Z, Mostov KE. A molecular switch for the orientation of epithelial cell polarization. *Dev Cell*. 2014;**31**(2):171–187.
22. Georgescu MM, Cote G, Agarwal NK, White CL 3rd. NHERF1/EBP50 controls morphogenesis of 3D colonic glands by stabilizing PTEN and ezrin-radixin-moesin proteins at the apical membrane. *Neoplasia*. 2014;**16**(4):365–374.e1–2.
23. Garbett D, LaLonde DP, Bretscher A. The scaffolding protein EBP50 regulates microvillar assembly in a phosphorylation-dependent manner. *J Cell Biol*. 2010;**191**(2):397–413.
24. Jeong J, VanHouten JN, Kim W, Dann P, Sullivan C, Choi J, Sneddon WB, Friedman PA, Wysolmerski JJ. The scaffolding protein NHERF1 regulates the stability and activity of the tyrosine kinase HER2. *J Biol Chem*. 2017;**292**(16):6555–6568.
25. Morales FC, Takahashi Y, Kreimann EL, Georgescu MM. Ezrin–radixin–moesin (ERM)-binding phosphoprotein 50 organizes ERM proteins at the apical membrane of polarized epithelia. *Proc Natl Acad Sci USA*. 2004;**101**(51):17705–17710.
26. Saotome I, Curto M, McClatchey AI. Ezrin is essential for epithelial organization and villus morphogenesis in the developing intestine. *Dev Cell*. 2004;**6**(6):855–864.
27. Sauvanet C, Wayt J, Pelaseyed T, Bretscher A. Structure, regulation, and functional diversity of microvilli on the apical domain of epithelial cells. *Annu Rev Cell Dev Biol*. 2015;**31**(1):593–621.

28. Bellizzi A, Malfettone A, Cardone RA, Mangia A. NHERF1/EBP50 in breast cancer: clinical perspectives. *Breast Care (Basel)*. 2010; **5**(2):86–90.
29. Cardone RA, Bellizzi A, Busco G, Weinman EJ, Dell'Aquila ME, Casavola V, Azzariti A, Mangia A, Paradiso A, Reshkin SJ. The NHERF1 PDZ2 domain regulates PKA-RhoA-p38-mediated NHE1 activation and invasion in breast tumor cells. *Mol Biol Cell*. 2007;**18**(5):1768–1780.
30. Dai JL, Wang L, Sahin AA, Broemeling LD, Schutte M, Pan Y. *NHERF* (Na^+/H^+ exchanger regulatory factor) gene mutations in human breast cancer. *Oncogene*. 2004;**23**(53):8681–8687.
31. Georgescu MM. NHERF1: molecular brake on the PI3K pathway in breast cancer. *Breast Cancer Res*. 2008;**10**(2):106.
32. Georgescu MM, Morales FC, Molina JR, Hayashi Y. Roles of NHERF1/EBP50 in cancer. *Curr Mol Med*. 2008;**8**(6):459–468.
33. Karn T, Ruckhäberle E, Hanker L, Müller V, Schmidt M, Solbach C, Gätje R, Gehrmann M, Holtrich U, Kaufmann M, Rody A. Gene expression profiling of luminal B breast cancers reveals NHERF1 as a new marker of endocrine resistance. *Breast Cancer Res Treat*. 2011;**130**(2):409–420.
34. Mangia A, Chiriatti A, Bellizzi A, Malfettone A, Stea B, Zito FA, Reshkin SJ, Simone G, Paradiso A. Biological role of NHERF1 protein expression in breast cancer. *Histopathology*. 2009;**55**(5): 600–608.
35. Maudsley S, Zamah AM, Rahman N, Blitzer JT, Luttrell LM, Lefkowitz RJ, Hall RA. Platelet-derived growth factor receptor association with Na^+/H^+ exchanger regulatory factor potentiates receptor activity. *Mol Cell Biol*. 2000;**20**(22):8352–8363.
36. Pan Y, Weinman EJ, Dai JL. Na^+/H^+ exchanger regulatory factor 1 inhibits platelet-derived growth factor signaling in breast cancer cells. *Breast Cancer Res*. 2008;**10**(1):R5.
37. Song J, Bai J, Yang W, Gabrielson EW, Chan DW, Zhang Z. Expression and clinicopathological significance of oestrogen-responsive ezrin–radixin–moesin-binding phosphoprotein 50 in breast cancer. *Histopathology*. 2007;**51**(1):40–53.
38. Morales FC, Hayashi Y, van Pelt CS, Georgescu MM. NHERF1/EBP50 controls lactation by establishing basal membrane polarity complexes with prolactin receptor. *Cell Death Dis*. 2012;**3**(9): e391.
39. Cheng S, Li Y, Yang Y, Feng D, Yang L, Ma Q, Zheng S, Meng R, Wang S, Wang S, Jiang WG, He J. Breast cancer-derived K172N, D301V mutations abolish Na^+/H^+ exchanger regulatory factor 1 inhibition of platelet-derived growth factor receptor signaling. *FEBS Lett*. 2013;**587**(20):3289–3295.
40. Du G, Gu Y, Hao C, Yuan Z, He J, Jiang WG, Cheng S. The cellular distribution of Na^+/H^+ exchanger regulatory factor 1 is determined by the PDZ-I domain and regulates the malignant progression of breast cancer. *Oncotarget*. 2016;**7**(20):29440–29453.
41. Du G, Hao C, Gu Y, Wang Z, Jiang WG, He J, Cheng S. A novel *NHERF1* mutation in human breast cancer inactivates inhibition by NHERF1 protein in EGFR signaling. *Anticancer Res*. 2016; **36**(3):1165–1173.
42. Antalffy G, Caride AJ, Pászty K, Hegedus L, Padanyi R, Strehler EE, Enyedi A. Apical localization of PMCA2w/b is enhanced in terminally polarized MDCK cells. *Biochem Biophys Res Commun*. 2011;**410**(2):322–327.
43. Padányi R, Xiong Y, Antalffy G, Lór K, Pászty K, Strehler EE, Enyedi A. Apical scaffolding protein NHERF2 modulates the localization of alternatively spliced plasma membrane Ca^{2+} pump 2B variants in polarized epithelial cells. *J Biol Chem*. 2010;**285**(41): 31704–31712.
44. Shenolikar S, Voltz JW, Minkoff CM, Wade JB, Weinman EJ. Targeted disruption of the mouse NHERF-1 gene promotes internalization of proximal tubule sodium-phosphate cotransporter type IIa and renal phosphate wasting. *Proc Natl Acad Sci USA*. 2002;**99**(17):11470–11475.
45. Liu L, Alonso V, Guo L, Tourkova I, Henderson SE, Almarza AJ, Friedman PA, Blair HC. Na^+/H^+ exchanger regulatory factor 1 (NHERF1) directly regulates osteogenesis. *J Biol Chem*. 2012; **287**(52):43312–43321.
46. Li M, Liu X, Robinson G, Bar-Peled U, Wagner KU, Young WS, Hennighausen L, Furth PA. Mammary-derived signals activate programmed cell death during the first stage of mammary gland involution. *Proc Natl Acad Sci USA*. 1997;**94**(7):3425–3430.
47. Zwick RK, Rudolph MC, Shook BA, Holtrup B, Roth E, Lei V, Van Keymeulen A, Seewaldt V, Kwei S, Wysolmerski J, Rodeheffer MS, Horsley V. Adipocyte hypertrophy and lipid dynamics underlie mammary gland remodeling after lactation. *Nat Commun*. 2018; **9**(1):3592.
48. RRID:AB_2198588, https://scicrunch.org/resolver/AB_2198588.
49. RRID:AB_823649, https://scicrunch.org/resolver/AB_823649.
50. RRID:AB_2084348, https://scicrunch.org/resolver/AB_2084348.
51. RRID:AB_2191505, https://scicrunch.org/resolver/AB_2191505.
52. RRID:AB_10649999, https://scicrunch.org/resolver/AB_10649999.
53. RRID:AB_2061585, https://scicrunch.org/resolver/AB_2061585.
54. RRID:AB_2191602, https://scicrunch.org/resolver/AB_2191602.
55. RRID:AB_2290063, https://scicrunch.org/resolver/AB_2290063.
56. RRID:AB_2108590, https://scicrunch.org/resolver/AB_2108590.
57. RRID:AB_397554, https://scicrunch.org/resolver/AB_397554.
58. RRID:AB_2801340, https://scicrunch.org/resolver/AB_2801340.
59. RRID:AB_2134736, https://scicrunch.org/resolver/AB_2134736.
60. RRID:AB_2243199, https://scicrunch.org/resolver/AB_2243199.
61. RRID:AB_10977236, https://scicrunch.org/resolver/AB_10977236.
62. RRID:AB_2801344, https://scicrunch.org/resolver/AB_2801344.
63. RRID:AB_2100309, https://scicrunch.org/resolver/AB_2100309.
64. RRID:AB_10949918, https://scicrunch.org/resolver/AB_10949918.
65. RRID:AB_2070042, https://scicrunch.org/resolver/AB_2070042.
66. RRID:AB_2203606, https://scicrunch.org/resolver/AB_2203606.
67. RRID:AB_2801345, https://scicrunch.org/resolver/AB_2801345.
68. VanHouten J, Sullivan C, Bazinet C, Ryoo T, Camp R, Rimm DL, Chung G, Wysolmerski J. PMCA2 regulates apoptosis during mammary gland involution and predicts outcome in breast cancer. *Proc Natl Acad Sci USA*. 2010;**107**(25):11405–11410.
69. Rudolph MC, McManaman JL, Hunter L, Phang T, Neville MC. Functional development of the mammary gland: use of expression profiling and trajectory clustering to reveal changes in gene expression during pregnancy, lactation, and involution. *J Mammary Gland Biol Neoplasia*. 2003;**8**(3):287–307.
70. Reinhardt TA, Lippolis JD. Mammary gland involution is associated with rapid down regulation of major mammary Ca^{2+}-ATPases. *Biochem Biophys Res Commun*. 2009;**378**(1):99–102.
71. Boras-Granic K, Dann P, Wysolmerski JJ. Embryonic cells contribute directly to the quiescent stem cell population in the adult mouse mammary gland. *Breast Cancer Res*. 2014;**16**(6):487.
72. Kouros-Mehr H, Slorach EM, Sternlicht MD, Werb Z. GATA-3 maintains the differentiation of the luminal cell fate in the mammary gland. *Cell*. 2006;**127**(5):1041–1055.
73. Russell TD, Jindal S, Agunbiade S, Gao D, Troxell M, Borges VF, Schedin P. Myoepithelial cell differentiation markers in ductal carcinoma in situ progression. *Am J Pathol*. 2015;**185**(11):3076–3089.
74. Franklin WA. Tissue binding of lectins in disorders of the breast. *Cancer*. 1983;**51**(2):295–300.
75. Bagchi S, Fredriksson R, Wallén-Mackenzie Å. In situ proximity ligation assay (pla). *Methods Mol Biol*. 2015;**1318**:149–159.
76. Donowitz M, Cha B, Zachos NC, Brett CL, Sharma A, Tse CM, Li X. NHERF family and NHE3 regulation. *J Physiol*. 2005;**567**(Pt 1):3–11.
77. Sarker R, Valkhoff VE, Zachos NC, Lin R, Cha B, Chen TE, Guggino S, Zizak M, de Jonge H, Hogema B, Donowitz M. NHERF1 and NHERF2 are necessary for multiple but usually separate aspects of basal and acute regulation of NHE3 activity. *Am J Physiol Cell Physiol*. 2011;**300**(4):C771–C782.

78. Brisken C, Kaur S, Chavarria TE, Binart N, Sutherland RL, Weinberg RA, Kelly PA, Ormandy CJ. Prolactin controls mammary gland development via direct and indirect mechanisms. *Dev Biol*. 1999;**210**(1):96–106.
79. Cui Y, Riedlinger G, Miyoshi K, Tang W, Li C, Deng CX, Robinson GW, Hennighausen L. Inactivation of Stat5 in mouse mammary epithelium during pregnancy reveals distinct functions in cell proliferation, survival, and differentiation. *Mol Cell Biol*. 2004; **24**(18):8037–8047.
80. Liu X, Robinson GW, Wagner KU, Garrett L, Wynshaw-Boris A, Hennighausen L. Stat5a is mandatory for adult mammary gland development and lactogenesis. *Genes Dev*. 1997;**11**(2):179–186.
81. Oakes SR, Rogers RL, Naylor MJ, Ormandy CJ. Prolactin regulation of mammary gland development. *J Mammary Gland Biol Neoplasia*. 2008;**13**(1):13–28.
82. Ikenouchi J, Hirata M, Yonemura S, Umeda M. Sphingomyelin clustering is essential for the formation of microvilli. *J Cell Sci*. 2013;**126**(Pt 16):3585–3592.